

# Structural stability and electrical properties of the chain structure of $\text{Ca}_2\text{CuO}_3$ under high pressure

G. M. Zhang,<sup>1,2</sup> W. J. Mai,<sup>1</sup> F. Y. Li,<sup>1</sup> Z. X. Bao,<sup>1</sup> R. C. Yu,<sup>1</sup> T. Q. Lu,<sup>2</sup> J. Liu,<sup>3</sup> and C. Q. Jin<sup>1,\*</sup><sup>1</sup>*Institute of Physics, Beijing High Pressure Research Center, Chinese Academy of Sciences, Beijing 100080, People's Republic of China*<sup>2</sup>*Department of Physics, Jilin University, Changchun 130023, People's Republic of China*<sup>3</sup>*Institute of High Energy Physics, Beijing High Pressure Research Center, Chinese Academy of Sciences, Beijing 100039, People's Republic of China*

(Received 11 July 2002; revised manuscript received 18 November 2002; published 9 June 2003)

*In situ* high-pressure energy dispersive x-ray-diffraction measurements on polycrystalline powder of  $\text{Ca}_2\text{CuO}_3$  with a Cu-O chain structure have been performed in a diamond-anvil cell (DAC) instrument using synchrotron radiation. The resistance versus pressure and capacitance versus pressure relationships up to 20 GPa have been studied simultaneously using the DAC technique at room temperature. The results showed that the structure of  $\text{Ca}_2\text{CuO}_3$  is stable under pressures up to 34 GPa. According to the Birch-Murnaghan equation of state, assuming  $B'_0=4$ , the bulk modulus  $B_0=165.4\pm 1.8$  GPa has been obtained. It is found that the resistance decreases continuously with increasing pressure up to 20 GPa, however, a sharp drop in the pressure range of 1.8~6 GPa is observed. Meanwhile the capacitance increases all along with the pressure and displays a steep jump at the same pressure range in which the resistance rapidly changes. This metallization phenomenon may be ascribed to an electronic structure transition induced by the pressure.

DOI: 10.1103/PhysRevB.67.212102

PACS number(s): 61.50.Ks, 61.66.Fn, 71.30.+h

## I. INTRODUCTION

Since the discovery of the high-temperature superconductor (HTSC),<sup>1</sup> the study of copper oxides has become very active. In a HTSC, the core structure is the conductive layers of  $[\text{CuO}_2]$ . At the same time, the Cu-O chains and imperfect  $[\text{CuO}_2]$  planes have important effects on the superconducting properties. For example, the orthorhombic structure of  $\text{YBa}_2\text{Cu}_3\text{O}_{7-\delta}$  has  $[\text{CuO}_4]$  square chains, aligned in the *b*-axis direction, which is crucial to its excellent properties.<sup>2</sup> Imperfect  $[\text{CuO}_2]$  planes and the  $[\text{CuO}_2]$  planes of the *n* infinite layer structure are all contained in the  $\text{CuBa}_2\text{Ca}_{n-1}\text{Cu}_n\text{O}_{2n+2+\delta}$  [i.e., Cu-12(*n*-1)*n*] homologous series.<sup>3</sup> Obviously, the imperfect  $[\text{CuO}_2]$  plane has great effects on the superconducting properties of the above compounds. The crystal structure of  $\text{Ca}_2\text{CuO}_3$  (Ref. 4) (Fig. 1) has corner-shared  $[\text{CuO}_4]$  squares in the same plane, which form a chain along the *b*-axis direction, similar to the chain of the orthorhombic structure  $\text{YBa}_2\text{Cu}_3\text{O}_{7-\delta}$ . The crystal structure of  $\text{Ca}_2\text{CuO}_3$  is similar to that of  $\text{La}_2\text{CuO}_4$  (Fig. 1), except that the oxygen ions between the Cu ions along the *a* axis are missed. As a result, chains of corner-shared  $\text{CuO}_4$  squares will extend in the *b*-axis direction. In high oxygen pressure (~5.0 GPa) syntheses,  $\text{Sr}_2\text{CuO}_3$ , with the same crystal structure as that of  $\text{Ca}_2\text{CuO}_3$ , can transform into tetragonal  $\text{Sr}_2\text{CuO}_{3+\delta}$ , which is isostructural to  $\text{La}_2\text{CuO}_4$ , and it becomes a HTSC.<sup>5</sup> High pressures have an overall effect on the structure and other properties of HTSC's. For example, the  $T_c$  of  $\text{HgBa}_2\text{Ca}_2\text{Cu}_3\text{O}_8$  is 133 K at ambient pressure, yet it can be raised up to 164 K under a high pressure of 30 GPa.<sup>6</sup> The ladder structure compound of  $\text{Ca}_{13.6}\text{Sr}_{0.4}\text{Cu}_{24}\text{O}_{41}$  shows no superconductivity at ambient pressure, but under 3~4 GPa it becomes a superconductor.<sup>7</sup> It is interesting to determine whether the Cu-O chains of  $\text{Ca}_2\text{CuO}_3$  can be changed into imperfect  $[\text{CuO}_2]$  planes simi-

lar to that in the Cu-12(*n*-1)*n* case through high-pressure treatment, and then the conductive  $[\text{CuO}_2]$  planes are formed, and how the transport properties will change with the pressure. In addition,  $\text{Ca}_2\text{CuO}_3$  is an important precursor material in high-temperature and high-pressure syntheses of superconductors. For example,  $\text{Ca}_2\text{CuO}_3$  is commonly used in the syntheses of the Cu-12(*n*-1)*n* homologous series.<sup>8</sup> So the investigation of the structural properties of  $\text{Ca}_2\text{CuO}_3$  under high pressure is also helpful to high-pressure syntheses of novel cuprate superconductors. Moreover,  $\text{Ca}_2\text{CuO}_3$  is a typical one-dimensional spin system with antiferromagnetic interactions due to the 180° Cu-O-Cu coupling,<sup>9</sup> and this one-dimensional system is widely considered to be closely

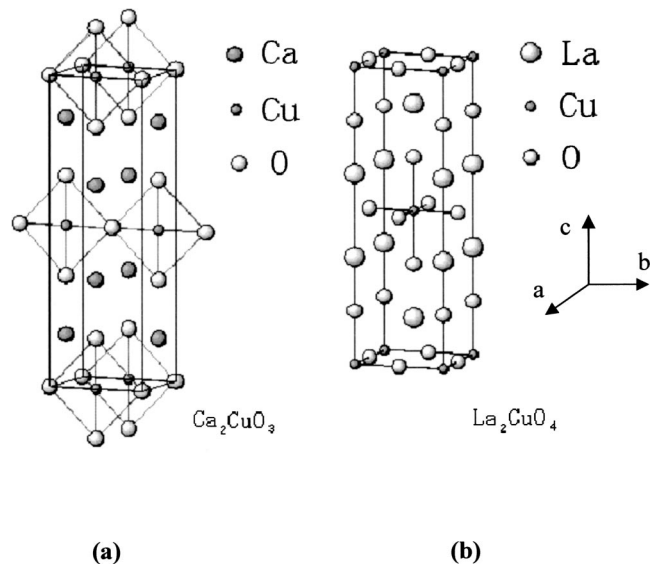


FIG. 1. The schematic representation of the crystal structures of (a)  $\text{Ca}_2\text{CuO}_3$  and (b)  $\text{La}_2\text{CuO}_4$ . The Cu-O coordination characters are highlighted.

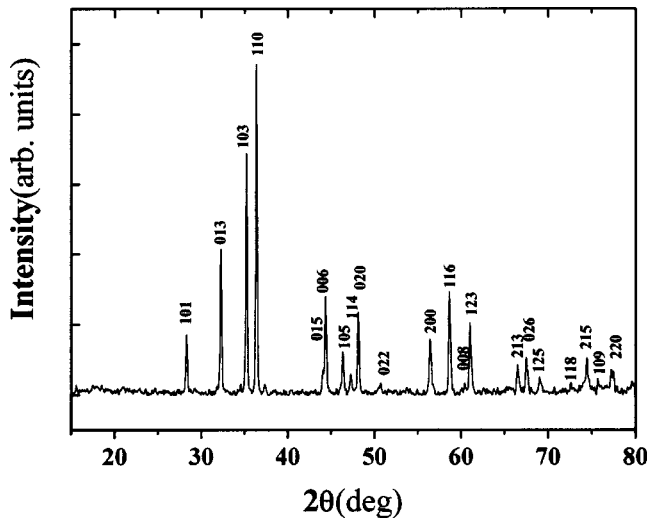


FIG. 2. The powder XRD pattern of the as-prepared  $\text{Ca}_2\text{CuO}_3$  sample.

related to the cuprate superconductors. The evolution of a structure under high pressure may affect its electronic configuration and consequently its transport properties. The *in situ* high-pressure electrical property research of  $\text{Ca}_2\text{CuO}_3$  has seldom been reported so far. We thus jointly carried out measurement of the simultaneous *in situ* resistance and capacitance versus pressure relationships, as well as the crystal structure change with applied pressure, using the energy dispersive x-ray-diffraction method, in order to obtain information on the crystal evolution and the corresponding electronic response with the pressure.

## II. EXPERIMENT

A sample of  $\text{Ca}_2\text{CuO}_3$  was prepared by the standard solid-state reaction method. Stoichiometric mixtures of high-purity oxides of CaO and CuO were thoroughly ground in an agate mortar for 1 h, and then sintered in air at  $980^\circ\text{C}$  for 24 h. The phase purity and crystal structure of the synthesized sample were examined by using a Rigaku x-ray diffractometer with a rotating anode at room temperature. Figure 2 shows the powder x-ray-diffraction (XRD) pattern, indicating that the sample is of a single-phase orthorhombic structure of  $\text{Ca}_2\text{CuO}_3$  with space group Immm, and the lattice parameters are  $a=0.3257(3)$ ,  $b=0.3776(9)$ , and  $c=1.223(6)$  nm.

The *in situ* high-pressure x-ray energy dispersive diffraction experiment on  $\text{Ca}_2\text{CuO}_3$  was carried out at room temperature in a diamond-anvil cell (DAC) using the white radiation from the synchrotron-radiation generator at the Beijing Synchrotron Radiation Laboratory. The size of the x-ray spot was  $120 \times 120 \mu\text{m}$ . The culet of the DAC was  $500 \mu\text{m}$ . The powder of the sample was loaded, with the Pt powder as the inner pressure standard, into a  $300\text{-}\mu\text{m}$  hole in a T301 stainless-steel gasket. The internal pressure of the DAC was calculated according to the equation of state of Pt.<sup>10</sup> In our experiments, the relation of energy and channel was  $E = 0.72453 + 0.00986 \cdot \text{chn}$ . According to the formula  $\sin \theta$

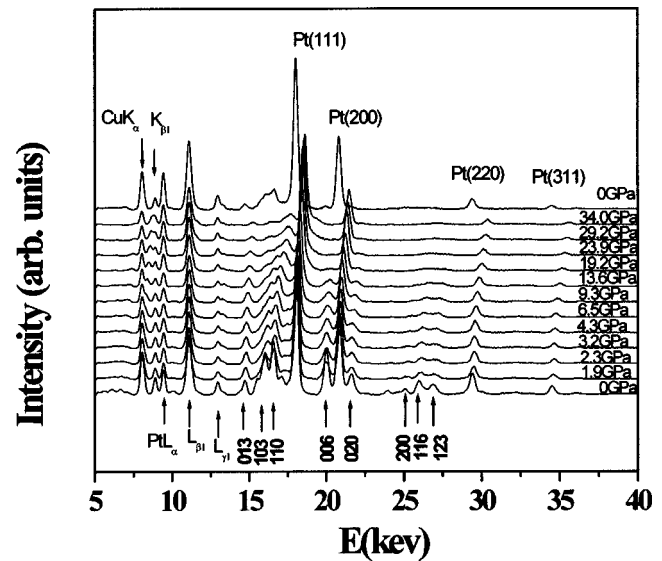


FIG. 3. The spectra of energy dispersive XRD of  $\text{Ca}_2\text{CuO}_3$  under various pressures. The fluorescent lines of the elements are assigned. The principal indices of the  $\text{Ca}_2\text{CuO}_3$  chain structure are indicated.

$= 61.9925/[d(\text{nm}) \cdot E(\text{keV})]$ , we got the exact value of  $\theta = 8.7303^\circ$ .

The *in situ* resistance and capacitance measurements were conducted simultaneously at room temperature with increasing pressure using the DAC. The culet of the diamond was  $\sim 500 \mu\text{m}$  in diameter. We used two parallel molybdenum sheets as electrodes. The molybdenum was selected due to its good mechanical and electrical performance under high pressure. The molybdenum electrodes were made by photoetching a base substrate composed of phenolic methyl. The electrode thickness was  $0.008\text{--}0.010$  mm, while the distance between the two electrodes was  $0.06\text{--}0.08$  mm. The sample was loaded into a hole centered at the base substrate. The electrodes and lead-in wires were fixed on a Plexiglas insulating mount and connected by silver conducting paste. The pressure was calibrated using the ruby fluorescent line. The data were recorded using an intelligent-type LCR high-resistance and capacitance instrument. The details of the experimental technique also can be found in Ref. 11.

## III. RESULTS AND DISCUSSION

The spectra of energy dispersive x-ray diffraction results of the  $\text{Ca}_2\text{CuO}_3$  sample under various pressures at room temperature are shown in Fig. 3. The ambient pressure spectra show the four peaks of Pt and the strongest peaks of the sample: (013), (103), (110), (006), (020), (200), (116), and (123). The maximum pressure applied was 34 GPa in our experiment. It is clear that all diffraction peaks of  $\text{Ca}_2\text{CuO}_3$  shift with increasing pressure. When the pressure returned to ambient, all the peaks came back to the original sites. In the whole course, except for a peak that appeared at about 10 GPa ( $E \approx 8.6$  keV), there was no other peak that could not be indexed with the  $\text{Ca}_2\text{CuO}_3$  orthorhombic lattice, so we can deduce that there is no crystal structure phase transition tak-

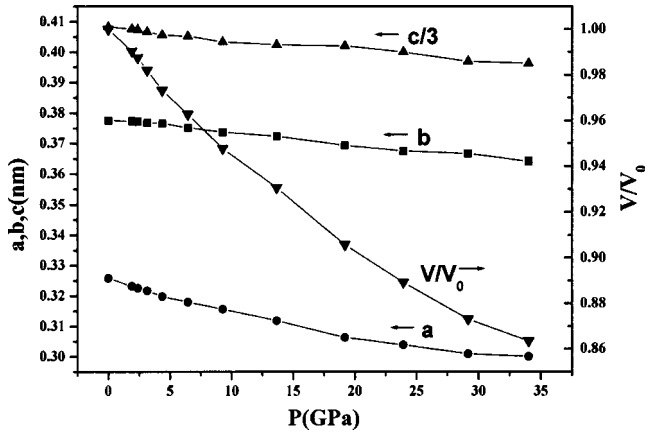


FIG. 4. Curves of the lattice parameters and volume compression versus pressure of the  $\text{Ca}_2\text{CuO}_3$  chain structure.

ing place in the pressure range of our experiment. To our best knowledge, the peak of  $E \approx 8.6$  keV, appearing at 10 GPa, has not been identified as yet. The peak is not a result of the first-order diffraction of the  $\text{Ca}_2\text{CuO}_3$  sample itself, but it may come from the second-order reflection of the  $\text{Ca}_2\text{CuO}_3$  or from the gasket reflection which overlaps with the Pt fluorescent peak at ambient condition. The lattice parameters of the sample were determined using a least-squares procedure based on the discernable main reflection indices of the sample indicated above. The changes of crystallographic parameters versus pressure and the equation of state at room temperature are plotted in Fig. 4. The diffraction data obtained at ambient pressure are slightly different from the standard diffraction spectra, so we adopt the initial volume at ambient pressure from our measured data.

Using the Birch-Murnaghan equation of state,

$$P(\text{GPa}) = 3/2 * B'_0 * [(V_0/V)^{7/3} - (V_0/V)^{5/3}] * \{1 - (3 - 3 * B'_0/4) * [(V_0/V)^{2/3} - 1]\},$$

we analyzed the data of volume compressibility versus pressure for  $\text{Ca}_2\text{CuO}_3$ . Assuming the first-order derivative to be  $B'_0 = 4$ , we obtain the bulk modulus  $B_0 = 165.4 \pm 1.8$  GPa. This value is comparable to that of ceramic oxides.

According to the band-structure calculation, the chain compound  $\text{Ca}_2\text{CuO}_3$ , which has an average  $\text{Cu}^{2+}$  valence state, is an antiferromagnetic insulator at ambient pressure.<sup>12</sup> We have conducted the studies of the *in situ* electrical property of the  $\text{Ca}_2\text{CuO}_3$  compound versus pressure at room temperature. The well-reproduced resistance versus pressure (R-P) and capacitance versus pressure (C-P) relationships for  $\text{Ca}_2\text{CuO}_3$  in several runs at room temperature are plotted in Fig. 5 with the y axis in logarithmic scale. As shown in Fig. 5, the resistance of the sample at the low-pressure range is quite high with an order of magnitude of  $10^4 \Omega$ . The resistance decreases continuously with the pressure loaded, but it drops sharply by almost one order of magnitude at pressure ranging from  $\sim 1.8$  to 6 GPa and thereafter decreases smoothly until 20 GPa with a resistance less than  $10^3 \Omega$ . The corresponding evolution of capacitance is measured simultaneously. A similar change appears in the capacitance as

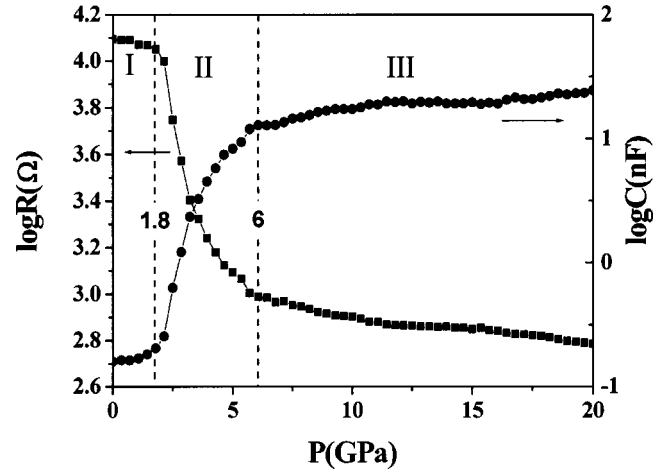


FIG. 5. Relationships of resistance and capacitance versus pressure for the  $\text{Ca}_2\text{CuO}_3$  chain structure. The left is for resistance while the right is for the capacitance. The y axis is plotted in a logarithmic scale.

shown in Fig. 5. The capacitance increases continuously in the low-pressure range but it jumps sharply in the range 1.8–6 GPa. It is clear that the changes of the R-P and C-P curves at room temperature are quite consistent with each other in the experimental pressure region.

According to the profile evolution of the two curves, the R-P and C-P changes can be divided into three regions. Region I corresponds to the initial change upon loading of the pressure, region II corresponds to the sharp change in the range 1.8–6 GPa, while region III corresponds to the smooth change in the high-pressure range.

The compactness of the polycrystalline sample under pressures always enhances the intergrain connection, which consequently leads to the improved conductance. In general, the energy gap in an insulator or semiconductor will decrease with increasing pressure, thus the resistivity is reduced. It is believed that the relatively smooth change of the R-P and C-P curves in the beginning (0–1.8 GPa) and the high-pressure (6–20 GPa) ranges result mainly from the aforementioned contribution. As for the consistent sharp changes in resistance and capacitance at 1.8–6 GPa, since the results of the high-pressure energy dispersive x-ray-diffraction measurements with synchrotron radiation show that the structure of  $\text{Ca}_2\text{CuO}_3$  is kept stable at pressures up to 34 GPa, we are inclined to believe that the sharp changes may be caused by the electronic structure transition, i.e., a metallization-like process of the parent antiferromagnetic insulating state of the  $\text{Ca}_2\text{CuO}_3$  chain structure upon the loading pressure. This is reinforced by the fact that the resistance and capacitance changes are almost reversible in the pressure loading and unloading cycling, indicating the electronic origination of the rapid change of the resistance. This metallization takes place in the compound without chemical doping, which is usually indispensable for reaching conducting cuprate compounds from the Mott-like parent state. Of course, more experimental evidence, such as that with optical investigation, would be helpful to further clarify the nature of the metallization of the  $\text{Ca}_2\text{CuO}_3$  chain structure under pressures.

## IV. SUMMARY

In summary, we have found through *in situ* synchrotron-radiation measurements that the structure of  $\text{Ca}_2\text{CuO}_3$  chain compound remains stable up to 34 GPa at room temperature. The bulk modulus and equation of state for  $\text{Ca}_2\text{CuO}_3$  are obtained under high pressures. The corresponding measurements of the R-P and C-P relationships show evidence that an electronic transition may occur at the pressure region of

$\sim 1.8\text{--}6$  GPa, which gives rise to a metallization-like change of the  $\text{Ca}_2\text{CuO}_3$  chain structure.

## ACKNOWLEDGMENTS

The authors are grateful to Professor L. C. Chen for assistance with the experiments. This work is financially supported by the National Natural Science Foundation of China, the Hundreds of Talents Program of the Chinese Academy of Sciences, and the State Key Program on Fundamental Research (Grant No. 2002CB613301).

\*Author to whom correspondence should be addressed.

- <sup>1</sup>J. G. Bednorz and K. A. Müller, *Z. Phys. B: Condens. Matter* **64**, 189 (1986).
- <sup>2</sup>W. I. F. David, W. T. A. Harrison, J. M. F. Gunn, O. Moze, A. K. Soper, P. Day, J. D. Jorgensen, D. G. Hinks, M. A. Beno, L. Soderholm, D. W. Capone II, I. K. Schuller, C. U. Segre, K. Zhang, and J. D. Grace, *Nature (London)* **327**, 310 (1987).
- <sup>3</sup>C.-Q. Jin, S. Adachi, X.-J. Wu, H. Yamauchi, and S. Tanaka, *Physica C* **223**, 238 (1994); X.-J. Wu, S. Adachi, C.-Q. Jin, H. Yamauchi, and S. Tanaka, *ibid.* **233**, 243 (1994); C.-Q. Jin, X.-J. Wu, S. Adachi, T. Tamura, T. Tatsuki, H. Yamauchi, S. Tanaka, and Z.-X. Zhao, *Phys. Rev. B* **61**, 778 (2000).
- <sup>4</sup>M. Hjorth and J. Hyltsoft, *Acta Chem. Scand.* **44**, 516 (1990).
- <sup>5</sup>Z. Hiroi, M. Takano, M. Azuma, and Y. Tateda, *Nature (London)* **364**, 315 (1993).
- <sup>6</sup>L. Gao, Y. Y. Xue, F. Chen, Q. Xiong, R. L. Meng, D. Ramirez, C. W. Chu, J. H. Eggert, and H. K. Mao, *Phys. Rev. B* **50**, 4260 (1994).
- <sup>7</sup>M. Uehara, T. Nagata, J. Akimitsu, H. Takahashi, N. Môri, and K. Kinoshita, *J. Phys. Soc. Jpn.* **65**, 2764 (1996).
- <sup>8</sup>C.-Q. Jin, S. Adachi, X.-J. Wu, and H. Yamauchi, in *Advances in Superconductivity* (Springer-Verlag, Berlin, 1995), Vol. VII, pp. 249–254; C.-J. Liu, C.-Q. Jin, and H. Yamauchi, *Phys. Rev. B* **53**, 5170 (1996).
- <sup>9</sup>K. M. Kojima, Y. Fudamoto, and M. Larkin, *Phys. Rev. Lett.* **78**, 1787 (1997).
- <sup>10</sup>N. C. Holmes, J. A. Moriarty, G. R. Gathers, and W. J. Nellis, *J. Appl. Phys.* **66**, 2962 (1989).
- <sup>11</sup>Z. X. Bao, V. H. Schmidt, and F. L. Johnson, *J. Appl. Phys.* **70**, 6804 (1991).
- <sup>12</sup>H. Rosner, H. Eschrig, R. Hayn, S.-L. Drechsler, and J. Málek, *Phys. Rev. B* **56**, 3402 (1997).